implicated in the catalytic mechanism (Hsu et al., 1977) since it lies so close to the active site carboxyl groups. Other spin-label studies are planned to probe possible conformational changes of Tyr-75 upon substrate and inhibitor binding.

References

Andreeva, N. S., & Gustchina, A. E. (1979) *Biochem. Biophys. Res. Commun. 87*, 32–42.

Bauer, D. R., Opella, S. J., Nelson, D. J., & Pecora, R. (1975) *J. Am. Chem. Soc. 97*, 2580–2582.

Cha, S. (1975) *Biochem. Pharmacol. 24*, 2177–2185.

Dill, K., & Allerhand, A. (1979) *J. Am. Chem. Soc. 101*, 4376–4378.

Dwek, R. A. (1973) *NMR in Biochemistry*, Clarendon Press, Oxford.

Dwek, R. A., Knott, J. C. A., March, D., McLaughlin, A. C., Press, E. M., Price, N. C., & White, A. I. (1975) *Eur. J. Biochem. 53*, 25–39.

Freed, J. H. (1976) in *Spin Labeling* (Berliner, L. J., Ed.) pp 53–132, Academic Press, New York.

Fruton, J. S. (1976) *Adv. Enzymol. Relat. Areas Mol. Biol. 44*, 1–36.

Haugland, R. P., & Stryer, L. (1967) *Conform. Biopolym., Pap. Int. Symp. 1*, 321.

Hsia, J. C., & Piette, L. H. (1969) *Arch. Biochem. Biophys. 129*, 296–307.

Hsu, I., Delbaere, T. J., James, M. N. G., & Hoffman, T. (1977) *Nature (London) 266*, 140–145.

Krugh, T. R. (1976) in *Spin Labeling—Theory and Applications* (Berliner, L. J., Ed.) pp 339–372, Academic Press, New York.

McCalley, R. C., Shimshick, E. J., & McConnell, H. M. (1972) *Chem. Phys. Lett. 13*, 115–119.

Morishima, H., Takita, T., & Umezawa, H. (1972) *J. Antibiot. 25*, 551–552.

Rich, D. H., & Sun, E. T. O. (1980) *Biochem. Pharmacol. 29*, 2205–2212.

Rich, D. H., Sun, E. T. O., & Singh, J. (1977) *Biochem. Biophys. Res. Commun. 74*, 762–767.

Rich, D. H., Sun, E. T. O., & Ulm, E. (1980) *J. Med. Chem. 23*, 27–33.

Schmidt, P. G. (1980) in *Frontiers in Protein Chemistry* (Liu et al., Eds.) pp 63–77, Elsevier/North-Holland, New York.

Shimshick, E. J., & McConnell, H. M. (1972) *Biochem. Biophys. Res. Commun. 46*, 321–327.

Subramanian, E., Liu, M., Swan, I. D. A., & Davies, D. R. (1979) in *Acid Proteases—Structure, Function and Biology* (Tang, J., Ed.) pp 33–41, Plenum Press, New York.

Sutton, B. J., Gettins, P., Givol, D., Marsh, D., Wain-Hobson, S., Willan, K. J., & Dwek, R. A. (1977) *Biochem. J. 165*, 177–197.

Tang, J. J. N. (1979) *Acid Proteases—Structure, Function and Biology*, Plenum Press, New York.

Tang, J. J. N., Sepulveda, P., Marciniszyn, J., Jr., Chen, K. C. S., Huang, W. Y., & Lanier, J. P. (1973) *Proc. Natl. Acad. Sci. U.S.A. 70*, 3437–3439.

Umezawa, H., Aoyogi, T., Morishima, H., Matzusaki, M., Hamada, H., & Takeuchi, T. (1970) *J. Antibiot. 23*, 259–262.

Workman, R. J., & Burkitt, D. W. (1979) *Arch. Biochem. Biophys. 194*, 157–164.

Yguerabide, J. (1972) *Methods Enzymol. 26 (part C)*, 528.

Direct Assignment of the Dihydrouridine-Helix Imino Proton Resonances in Transfer Ribonucleic Acid Nuclear Magnetic Resonance Spectra by Means of the Nuclear Overhauser Effect†

Dennis R. Hare‡ and Brian R. Reid*

ABSTRACT: The NMR resonances from the hydrogen-bonded ring NH protons in the dihydrouridine stem of *Escherichia coli* $tRNA_1^{Val}$ have been assigned by experiments involving the nuclear Overhauser effect (NOE) between adjacent base pairs. Irradiation of the 8–14 tertiary resonance produced a NOE to base pair 13. Irradiation of the CG13 ring NH produced NOEs to base pairs 12 and 14. Similarly, base pair 12 was shown to be dipolar coupled to 11 and 13, and base pair 11 was found to be coupled to 10 and 12. These sequential connectivities led to the assignment of CG13 at −13.05 ppm, UA12 at −13.84 ppm, CG11 at −12.23 ppm, and GC10 at −12.60 ppm. The results are compared with previous, less direct assignments for these four base pairs and with the expected proton positions from the crystal structure coordinates for this helix.

High-resolution NMR[1] is potentially the most informative spectroscopic tool for studying the molecular structure and dynamics of transfer RNA in solution (Crothers & Cole, 1978; Schimmel & Redfield, 1980). Although several regions of the ^1H NMR spectrum containing different types of protons have been studied in several laboratories (Kastrup & Schmidt, 1975, 1978; Kan et al., 1977; Robillard et al., 1977a,b; Schmidt & Edelheit, 1981), the most useful region of the NMR spectrum of tRNA is probably the extreme low-field spectrum between

† From the Chemistry Department and Biochemistry Department, University of Washington, Seattle, Washington 98195. *Received October 19, 1981.* This work was supported by research grants from the National Institute of General Medical Sciences (GM28764), the National Science Foundation (PCM-8140603), and the American Cancer Society (NP-191D) and by instrumentation grants from the National Science Foundation (PCM80-18053) and from the National Institutes of Health, Department of Health, Education and Welfare (MG28764-01S1).

‡ D.H. is a predoctoral student in the graduate program of the Biochemistry Department, University of California, Riverside, CA 92521.

[1] Abbreviations: tRNA, transfer ribonucleic acid; NMR, nuclear magnetic resonance; NOE, nuclear Overhauser effect; DSS, 4,4-dimethylsilapentane-1-sulfonate; D, dihydrouridine; s^4U, 4-thiouridine; Ψ, pseudouridine.

0006-2960/82/0421-1835$01.25/0

−10 and −15 ppm. This region contains imino or ring NH protons hydrogen bonded between complementary base pairs and there is only one such proton per base pair [for a recent review, see Reid (1981)]. These low-field resonances were detected several years ago by Kearns & Shulman (1974), and because they are exchangeable, the very fact of their observation adds kinetic or dynamic information to the structural information encoded in their chemical shifts.

Most normal tRNAs contain 26–28 ring NH resonances in their low-field spectra (Reid et al., 1975, 1977; Daniel & Cohn, 1975), but progress in studying tRNA base-pair hydrogen bonding by low-field NMR spectroscopy has been held up by the lack of rigorous, unequivocal assignments for these resonances. Several strategies have been used in attempting to solve the assignment problem, but the results are often contradictory. Empirical ring-current shift calculations have been employed based on experimental spectra (Shulman et al., 1973; Reid et al., 1979) as well as theoretical ring-current shift calculations based on the X-ray crystallographic coordinates (Robillard et al., 1976; Geerdes & Hilbers, 1977; Kan & Ts'o, 1977). Individually dissected hairpin helices have been examined in the hope that the intact molecule spectrum is the sum of the component parts (Lightfoot et al., 1973; Kearns & Shulman, 1974; Reid et al., 1979). All of the above methods suffer from having to make assumptions about helix geometry in solution as well as inherent ring NH chemical shifts in water.

Among the observed 26–28 imino protons there are approximately 6 that are derived from tertiary base pairs involved in the three-dimensional folding of tRNA (Reid et al., 1975, 1977, 1979), and some of these tertiary base pairs present a uniquely manipulatable chemical handle by which 1 or 2 confident assignments can be made. One particular example is the thiolated uridine at residue 8 in most bacterial tRNAs; the ring NH of the s^4U8–A14 tertiary base pair resonates at the extremely deshielded position of −14.9 ppm as demonstrated by chemical dethiolation or NMR analysis of biologically underthiolated tRNA species (Reid et al., 1975, 1979; Daniel & Cohn, 1975; Wong et al., 1975). This particular tertiary assignment is now virtually certain, and it enjoys a much higher confidence level than the large majority of the secondary Watson–Crick assignments.

Perhaps the most reliably assigned secondary resonances are those of the nonstandard GU base pair often found in tRNA. "Wobble" GU pairs contain *two* hydrogen-bonded ring NH protons that are strongly dipolar coupled due to their close proximity (<3Å). Johnston & Redfield (1978) were able to identify the two ring NHs of GU4 in yeast $tRNA^{Phe}$ from this dipolar coupling by means of their large (20–40%) mutual nuclear Overhauser effects (NOE); application of this technique to other tRNAs led to the assignment of both imino protons of GU50 in *Escherichia coli* $tRNA_1^{Val}$ and of UG50 in *E. coli* $tRNA^{fMet}$ (Hurd & Reid, 1979b; Johnston & Redfield, 1979). Independent corroboration that the two ring NHs exhibiting large reciprocal NOEs are derived from the GU pair comes from studies of different tRNAs containing a single GU pair in identical environments (K. A. Jones and B. R. Reid, unpublished data).

The NOE is a dipole–dipole phenomenon in which magnetization is transferred through space from one proton to an adjacent proton (Noggle & Schirmer, 1971). In polymers NOEs are negative; they are dominated by cross relaxation and reflect the saturation of adjacent protons when a given proton is saturated by preirradiation. The efficiency of this cross saturation falls off as the sixth power of distance, and the size of the NOE for a particular proton depends on how many other protons are also close enough to be dipolar coupled to the irradiated proton (Bothner-By, 1979). In proteins the NOE is experimentally detectable out to distances of 3.5–4 Å (Poulsen et al., 1980; Dubs et al., 1979). Johnston & Redfield (1981) have calculated that their observed NOEs of ca. 30% correspond to a distance separation of ca. 2.8 Å between G N1-H and U N3-H in the yeast $tRNA^{Phe}$ GU4 base pair. Thus, at present the most definitive assignments are those of the s^4U8–A14 tertiary base pair and the wobble GU secondary base pair assigned by NOE.

In general, the NOE falls off to undetectable levels at a distance around 4 Angstroms between protons. In RNA, the vertical separation between base planes in the helical stacks results in relatively large distances between protons of adjacent base pairs, reducing their mutual NOEs below detectability in all but a few exceptional cases. Tropp & Redfield (1981) selectively saturated the methyl protons of the common thymine found at residue 54 in tRNA and observed a NOE to a ring NH resonating near −10.7 ppm in yeast $tRNA^{Phe}$ and *E. coli* $tRNA_1^{Val}$. They assigned this ring NH to N1-H (not hydrogen bonded) of the adjacent Ψ55 residue based on measurements from the crystal structure indicating that this was the only ring NH within 4 Å of the thymine methyl group; this assignment was confirmed by the intraresidue NOE from this proton to Ψ55 C6-H. Using this same approach, Johnston & Redfield (1981) assigned the ring NH of m^2GC10 in yeast $tRNA^{Phe}$ at −12.63 ppm based on the observed NOE from the m^2G10 methyl protons; however, this is an intra base pair rather than an inter-base-pair NOE. Usually imino–imino NOEs from nearest neighbors are beyond the limits of detection due to the distance (at least 3.8 Å) between ring NHs of adjacent base pairs in a normal helix. However, the first suggestion of a NOE between imino protons of nearest-neighbor base pairs came from Johnston & Redfield's (1981) study of the GU4 imino protons in yeast $tRNA^{Phe}$; they noticed that saturation of either the G or U imino proton produced a weak NOE at −13.88 ppm which they tentatively concluded might be the imino proton of the adjacent base pair AU5. We have confirmed this result and observed that, in general, the NOE to a nearest-neighbor Watson–Crick imino proton is stronger when the saturated donor ring NH is from a GU wobble pair; the reason for this is that helix distortion from wobbling places the GU imino protons closer to the nearest neighbor ring NH and, in addition, saturation of either of the GU imino protons heavily cross saturates the other, resulting in two donor sources of saturation for cross relaxation. Thus, in a series of different tRNAs we find that GU imino protons, regardless of their position in the tRNA, give quite strong (5–10%) NOEs to the imino protons of the nearest base pair.

In a very recent elegant application of the NOE method Roy & Redfield (1981) made use of the somewhat atypical base-pair sequence in the D helix of yeast $tRNA^{Asp}$ which has GU10 at one end, ΨG13 at the other end, and two intervening AU pairs in positions 11 and 12. From a combination of C8 deuteration, to distinguish Hoogsteen pairs, and NOE connectivities, they were able to assign the imino protons of GU10, UA11, and UA12; the NOE from, and to, U8–A14 independently led to the assignment of ΨG13. Thus, although UA12 and ΨG13 were not experimentally connected by NOE, Roy and Redfield were able to establish the identity of all the imino proton markers in the entire $tRNA^{Asp}$ D stem. Encouraged by this demonstration of ring NH NOEs between adjacent base pairs we reasoned that with the increased sensitivity of 500 MHz, we might be able to detect the NOE

between imino protons of adjacent base pairs in a normal helix of Watson–Crick pairs devoid of wobble pairs and thus sequentially assign the resonances by direct NOE connectivity from some reference point. In the present paper we have examined the CG13-UA12-CG11-GC10 D helix of *E. coli* $tRNA_1^{Val}$. We report the direct assignment of the CG13 ring NH via the NOE from the independently assigned s^4U8–A14 tertiary base pair. We also extended the assignments by NOE from 13 to 12, from 12 to 11, and from 11 to 10, resulting in complete assignment of all the D-helix low-field protons of *E. coli* $tRNA_1^{Val}$. These direct assignments from dipolar coupling are now virtually unambiguous in that they involve no prior assumptions about unshifted resonance positions or helix geometry. The resonance position of CG13 was found to differ markedly from its previous assignment based on assumptions which now prove to be unjustified.

Materials and Methods

Transfer RNA. *E. coli* $tRNA_1^{Val}$ was purified to homogeneity from crude tRNA by a three-column chromatographic procedure involving BD-cellulose, DEAE-Sephadex A-50, and Sepharose 4B as described previously (Reid et al., 1977, 1979). The final material accepted 1800 pmol of valine/A_{260} and was stored as a lyophilized powder after dialysis against distilled water.

NMR Spectra. Between 7 and 8 mg of pure, lyophilized *E. coli* $tRNA_1^{Val}$ was dissolved in 0.35 mL of 10 mM sodium cacodylate–1 mM Na_4EDTA–15 mM magnesium chloride–100 mM NaCl at pH 7.0 to give an 0.85 mM tRNA solution which was transferred to a Wilmad CP 528 NMR tube. Between NMR experiments the sample was slowly frozen by laying the NMR tube on its side in a −20 °C freezer. NMR spectra (500 MHz) were obtained on a Bruker WM500 pulsed FT NMR spectrometer at 23 °C, except where stated otherwise. Spectra were collected in 8K channels by using a phase-shifted Redfield 214 pulse with a total pulse length of 205 μs and a carrier frequency offset of 4750 Hz from the water resonance (acquisition time, 0.28 s; relaxation delay, 0.1 s). Usually 1000 pulses were signal averaged for 6–7 min in an Aspect 2000 computer, Fourier transformed, phase corrected, and directly plotted on 8 × 11 in. plain white paper after base-line correction. Chemical shifts are reported as ppm from DSS (4,4-dimethylsilapentane-1-sulfonate).

For the NOE experiments, a given peak of interest was selectively saturated by gated irradiation at that frequency, by using just enough decoupler power to almost saturate the resonance in 0.1 s. If one of a pair of closely spaced peaks was to be saturated, it was irradiated slightly off the exact top of the peak on the side away from the adjacent peak; this gave greater selectivity by reducing irradiation spillover to the neighboring peak. A 0.3-ms delay was inserted between switching off the preirradiation and triggering the observe–acquisition pulse sequence. For monitoring the time dependence of the NOE buildup, we used preirradiation times of 0.1, 0.2, 0.4, 0.6, and 1.0 s. Single time NOEs were performed with either 0.2 or 0.4 s of preirradiation. The NOE data were collected directly, by interleaving, as NOE difference spectra by using difference Fourier techniques (Redfield & Kunz, 1979). Usually eight pulses irradiated on the resonance and eight pulses irradiated off resonance were interleaved in an alternating cycle with memory negation to generate the difference FID which was Fourier transformed to directly generate the difference spectrum in the frequency domain. For small NOEs around the 2% range, 4000–8000 pulses were sufficient to unambiguously reveal the NOE above background noise in the transformed difference spectrum.

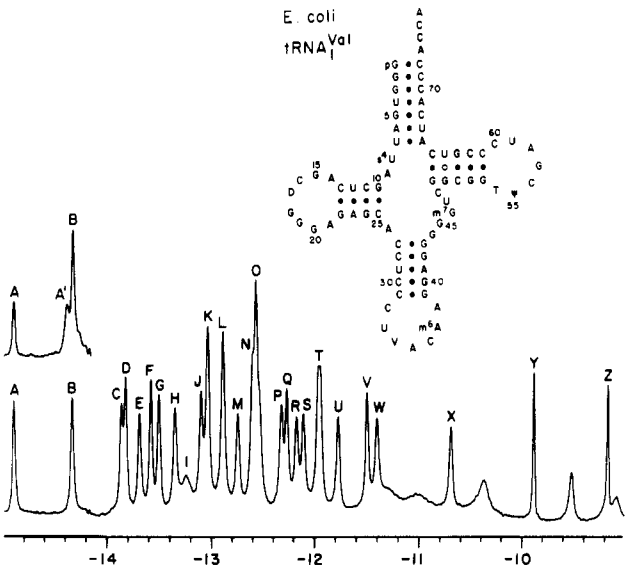

FIGURE 1: 500-MHz FT NMR spectrum of 0.85 mM *E. coli* $tRNA_1^{Val}$ at 27 °C under partially limiting magnesium ion conditions (see the text and Materials and Methods). The spectrum was obtained in 6 min of signal averaging with a Redfield 214 observe pulse and was slightly resolution enhanced by mixed exponential–Gaussian (20% Gaussian) apodization of the FID. Upper left: The spectrum between −14 and −15 ppm of an identically prepared sample containing 50% s^4U and 50% U at residue 8. Half of peak A is now 0.55 ppm upfield (peak A′).

Results

The low-field ring NH spectrum of 0.85 mM *E. coli* $tRNA_1^{Val}$ at 500 MHz is shown in Figure 1. Each base pair in the molecule generates only one hydrogen-bonded ring NH, and the 28 protons in peaks A to W (including the partially melted base pair I) indicate the presence of 27 base pairs (including GU50) with long lifetimes on the millisecond time scale; peak I reappears as a discrete resonance upon further lowering the temperature. Peaks X and Y and the two peaks at −10.4 and −9.5 ppm probably represent ring NHs that are not base paired but are slowed down in their water exchange rate because of partial accessibility to solvent. Peak Z is a carbon proton resonance from C8-H of m^7G46 (Hurd & Reid, 1979a,b). This spectrum was obtained on a sample after 5–6 days of storage at −20 °C and several freeze–thaw cycles. Although the sample was originally made up in the presence of excess magnesium, the spectrum is remarkably similar to the intermediate magnesium spectrum reported earlier at 360 MHz (Reid et al., 1979). It may well be that freezing and storage at −20 °C causes limited, visually imperceptible precipitation of magnesium ion at pH 7. Also shown in the upper left inset of Figure 1 is the −14- to −15-ppm region of a sample of the same tRNA species which was found by chemical and UV spectroscopic analysis to contain 50% s^4U and 50% U at residue 8. The fact that half of peak A has now moved upfield to −14.35 ppm corroborates the previously established assignment of peak A to the s^4U8–A14 tertiary base pair (Reid et al., 1975; Daniel & Cohn, 1975, 1976; Wong et al., 1975; Hurd & Reid, 1979a). The deshielding of the ring NH of s^4U compared to uridine is the reason why this hydrogen bond resonates at lower field than normal base pairs (Hurd & Reid, 1979a).

The fact that the resonance at −14.9 ppm can be so readily assigned to the 8–14 tertiary base pair, and that this assignment has been corroborated in several laboratories, made peak A the logical starting point for our attempts to assign the ring NHs of adjacent base pairs via ring NH–ring NH NOEs between peaks in the low-field spectrum. Since the 8–14

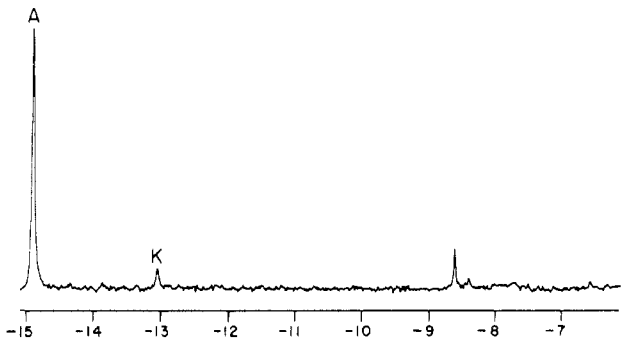

FIGURE 2: Difference NOE spectrum from saturation of the ring NH of s^4U8–A14. Peak A was selectively irradiated to saturation for 0.4 s. The 4000 pulse difference FID was collected by alternating 8 pulses on peak A and 8 pulses of off resonance base-line irradiation and then directly Fourier transformed into the frequency domain. The intensity of peak A in the difference spectrum corresponds to a single proton with a signal-to-noise ratio of 55 (0.85 mM tRNA). The narrow aromatic CH NOE at −8.65 ppm is the nearby C8-H of A14 which is a resolved single proton in the aromatic spectrum (see Figure 3).

tertiary base pair is stacked upon the four base pair D stem in the crystal structure of yeast $tRNA^{Phe}$ (Rich & RajBhandary, 1976; Kim, 1976; Jack et al., 1976), our hope was to sequentially assign these four secondary base pairs step by step using direct NOEs to the adjacent nearest neighbor.

Figure 2 shows the effect of irradiating the 8–14 base pair resonance to saturation for 0.4 s. The difference spectrum readily reveals a NOE to a narrow aromatic CH at −8.65 ppm and a smaller NOE to a broader amino proton at −8.4 ppm. Because of the steep distance dependence of the dipolar NOE phenomenon ($1/r^6$), these resonances are almost certainly A14 C8-H and the A14 amino group within the 8–14 base pair since these are the only protons closer than 3 Å from the ring NH of residue 8 in the crystal structure (see Table I). Rotation about the C–N bond and the faster relaxation of amino protons both would contribute to attenuating the NOE effect on amino protons compared to fixed aromatic CH protons. A more important result is that saturation of s^4U8 N3-H also cross relaxes another ring NH at −13.05 ppm; careful alignment, as well as NOE experiments in the reverse direction, indicates that it is peak K that is dipolar coupled to the ring NH of s^4U8. Qualitatively this could be either CG13 or the tertiary base pair G15–C48, both of which are adjacent to the s^4U8–A14 base pair. According to the refined crystal coordinates (Sussman et al., 1978), the ring NH of CG13 (G22 N1-H) is within 3.1 Å of U8 N3-H whereas G15 N1-H is 4.6 Å away. The NOE at 3.1 Å should be more than 10 times greater than that at 4.6 Å, strongly indicating that peak K is in fact the ring NH of CG13. This reasoning is based on analogy with the crystal structure of yeast $tRNA^{Phe}$. *E. coli* $tRNA_1^{Val}$ has the same folding potential as yeast $tRNA^{Phe}$ (Klug et al., 1974; Kim et al., 1974), and its D stem differs only in the thiolation of uridine-8 and the absence of a methyl group on G10. Although barely perceptible in Figure 2 (0.4-s saturation), further experiments in which the NOE was driven by saturating peak A for periods approaching 1 s produced additional very weak NOEs to imino protons D, H, and R (data not shown). These very weak, higher order effects result from the spin-diffusion phenomenon discussed later.

An additional diagnostic feature in these experiments is the chemical nature of the NOE-related protons in the −7- to −9-ppm region of the spectrum which contains a mixture of amino protons (from A, G, and C bases) and aromatic CH protons. Because of their close proximity, the largest NOEs upon irradiating a given resonance are to other protons within the same base pair. In a Watson–Crick GC pair, the nearest

Table I: Distance to Surrounding Protons from the Ring NH of Each Base Pair in the D Helix of tRNA[a]

base pair	ring NH	distance (in A) to surrounding protons[c]
14–8	U8 N3-H	2.6, 4.3 [A14 NH_2]
		2.9 [A14 C8-H]
		3.1[b] [G22 N1-H (bp 13)]
		3.7, 4.5 [C13 NH_2 (bp 13)]
		4.0, 4.8 [G22 NH_2 (bp 13)]
		4.3 [U8 C5-H]
		4.6[b] [G15 N1-H (bp 15)]
13–22	G22 N1-H	2.3, 3.4 [G22 NH_2]
		2.6, 4.0 [C13 NH_2]
		3.1[b] [U8 N3-H (bp 14)]
		3.4, 3.7 [A23 NH_2 (bp 12)]
		4.1, >5 [A14 NH_2 (bp 14)]
		4.4 [A14 C8-H (bp 14)]
		4.3, >5 [G46 NH_2 (46-22-13)]
		4.7[b] [U12 N3-H (bp 12)]
12–23	U12 N3-H	3.0 [A23 C2-H]
		2.6, 4.0 [A23 NH_2]
		3.8[b] [G24 N1-H (bp 11)]
		4.3 [U12 C5-H]
		4.5 [C13 C6-H (bp 13)]
		4.7[b] [G22 N1-H (bp 13)]
		4.4, >5 [C11 NH_2 (bp 11)]
11–24	G24 N1-H	2.3, 3.4 [G24 NH_2]
		2.4, 3.9 [C11 NH_2]
		3.4[b] [G10 N1-H (bp 10)]
		3.8[b] [U12 N3-H (bp 12)]
		3.8, 4.9 [G10 NH_2 (bp 10)]
		4.1, 4.7 [C25 NH_2 (bp 10)]
		4.1, >5 [A23 NH_2 (bp 12)]

[a] The C, N, O, and P coordinates of the reciprocal space refined crystal structure of yeast $tRNA^{Phe}$ were used (Sussman et al., 1978); *E. coli* $tRNA_1^{Val}$ contains the same sequence in the D stem. Proton coordinates were generated by a computer program using the known C–H and N–H bond distances and angles (D. Hare, unpublished). [b] Ring NH of adjacent base pair. [c] Surrounding protons in brackets.

protons to the ring NH are from the G amino group and the C amino group. These amino protons have relatively broad line widths (similar to ring NH line widths) due to the extra relaxation from the nitrogen. On the other hand, in a Watson–Crick AU pair one of the nearest protons to the ring NH is the adenine aromatic C2-H proton which has a remarkably narrow line width (Schmidt & Edelheit, 1981). Even for Hoogsteen AU pairs, one of the closest proton neighbors to the ring NH is an aromatic carbon proton, in this case C8-H of adenine (see Table I). Redfield's group has used deuteration of C8-H's to distinguish Watson–Crick AU pairs from Hoogsteen AU pairs (Sanchez et al., 1980). Thus, regardless of whether the AU pair is of the Hoogsteen or Watson–Crick type, irradiation of an AU ring NH can easily be distinguished from that of a GC pair; the AU ring NH generates a narrow CH NOE in the −9- to −7-ppm region whereas the GC pair does not. This is a useful diagnostic tool when irradiating unknown ring NH lines in the spectral region where AU and GC ring NHs overlap.

Proceeding on the basis that peak K is in fact CG13, this peak was next selectively saturated by irradiating on the slightly upfield side to avoid exciting peak J. As shown in Figure 3, the NOE to the upfield aromatic region involves only broad amino protons, indicating that peak K contains only GC base pairs. In the low-field spectrum the expected reverse NOE back to peak A (the 8–14 pair) was observed as well as a new NOE to peak D at −13.84 ppm. This chemical shift is highly indicative of an AU pair and agrees well with our previous assignment of UA12 on less direct evidence (Reid et al., 1979). Although highly suggestive, the evidence that

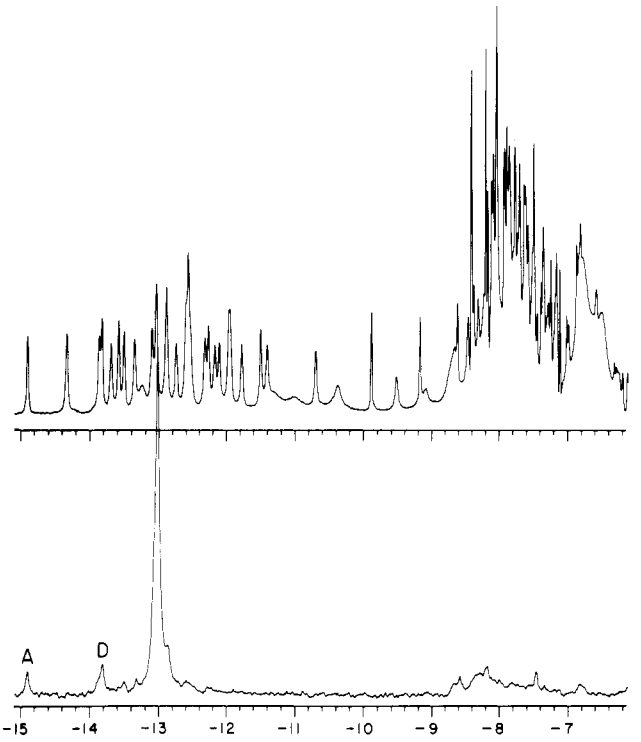

FIGURE 3: NOE difference spectrum produced by selectively saturating peak K for 0.4 s. Cross saturation of peaks A and D is evident. The absence of any appreciable CH NOE in the upfield region indicates that neither of the base pairs in peak K is an AU pair (Sanchez et al., 1980). Saturation is just beginning to appear in the resolved C8-H signal of A14 at −8.6 ppm (see Figure 2). The upper spectrum is a reference 27 °C unirradiated spectrum scaled identically in the *x* axis but scaled down 2.6-fold in the *y* axis. The upfield aromatic portion of the spectrum has a suppressed overall intensity because (a) the pulse repetition cycle was shorter than the CH T1 value and (b) it is closer to the zero-excitation null at −4.6 ppm in the tailored 214 observation pulse.

cross relaxation of peak D by peak K is a NOE from CG13 to UA12 is not completely unambiguous. Peak K contains two base pairs, and it could be the other GC pair, rather than CG13, that is coupled with peak D; the only firm conclusions at this stage are that both base pairs in peak K are GC pairs, one of them is CG13, one of them is very close to base pair D, and D is probably an AU pair by virtue of its chemical shift.

To shed more light on this, we next irradiated peak D on the upfield side to avoid saturating peak C and also monitored the time dependence of this NOE in an experiment exactly analogous to the truncated driven NOE technique used on proteins (Wagner & Wuthrich, 1979). The results are shown in Figure 4. The rapid NOE to a narrow CH resonance at −7.55 ppm (A23 C2-H) establishes that peak D is definitely an AU base pair. At early time points up to 0.2 s, two ring NH NOEs are observed, one back to peak K and one to peak Q. At later times beyond 0.4 s, a third NOE to peak N begins to appear. Peak K has already been shown to contain two GC pairs, one of which is CG13, and by virtue of its resonance position, peak Q is almost certainly a GC pair. It was initially difficult to unambiguously identify which peak at −12.3 ppm was the NOE receptor because at 23 °C, where the NOE studies were carried out, peaks P and Q are virtually coalesced. However, repeating the experiment at slightly higher temperatures where P and Q partially resolve (see Figure 1) establishes that it is Q, and not P, that is spatially connected to D. We interpret the NOEs from peak D to peaks K and Q to reflect coupling from UA12 to CG13 and to CG11, respectively, and the cross relaxation of peak N at later times to reflect a slower, higher order NOE from UA12 to GC10

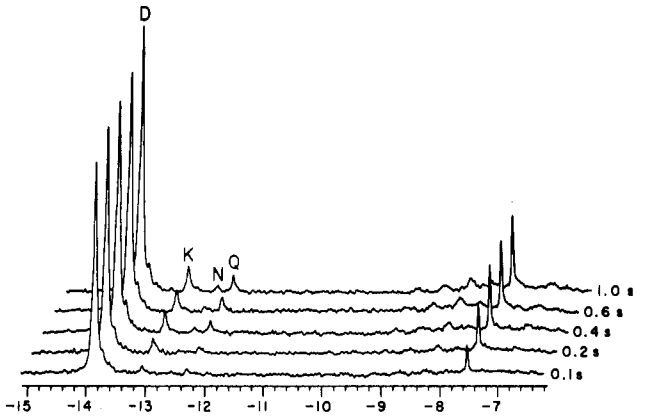

FIGURE 4: Time dependence of the driven NOE produced by saturating peak D. At 0.1 and 0.2 s of saturation, peaks K and Q are the only ring NHs to be cross saturated. At 0.4 s and longer, saturation begins to appear in peak N. The rapid appearance of a narrow CH NOE at −7.55 ppm (A23 C2-H) indicates peak D is an AU base pair.

via CG11. In such higher order NOEs the saturation from UA12 is passed along "second hand" to GC10 by a domino effect chain reaction involving mutual spin flipping of the amino, ring NH, or CH protons of CG11 as intermediaries; this process is known as "spin diffusion" (Kalk & Berendsen, 1976; Wagner & Wuthrich, 1979). Thus, we conclude that peak Q is CG11 and peak N is probably GC10.

Although the dipolar coupling of proton D to its two nearest neighbors K and Q adds weight to our assignment of D, K, and Q to UA12, CG13, and CG11, respectively, it has not completely resolved the problem caused by an additional base pair residing with CG13 in peak K. It is still possible that we took the wrong exit from peak K after entering this "crossroads" from peak A; i.e. peak D might possibly be the neighbor of the other base pair in peak K. If this were true, then base pair D, instead of being the next-to-nearest neighbor of the tertiary 8–14 peak A, could be far removed from CG13 in some other part of the molecule. Strong evidence that this is not the case came from driving the NOE from s^4U8–A14 to longer time periods. When peak A was saturated for periods approaching 1 s, a higher order NOE to peak D at −13.84 ppm (as well as peaks H and R) became detectable (this second-order or third-order NOE is just beginning to appear at 0.4 s upon close inspection of Figure 2). In this experiment, energy is pumped into the system exclusively through tertiary base pair 14 (s^4U8–A14), ensuring that only CG13 and not the "other proton" in peak K is cross saturated. Because peak D can be partially saturated when only the CG13 component in peak K is cross saturated by irradiating peak A, we can establish the connectivity A–K–D. Thus peak D can be spatially connected to peak A through peak K and must be the next-to-nearest neighbor of base pair 14; this establishes that peak D is in fact UA12. Peaks H and R are probably m^7G46 (hydrogen bonded to CG13) and G15–C48, respectively; they are both quite close to s^4U8–A14 and will be the subject of a separate communication.

Continuing down the helix, the results of selectively saturating CG11 at −12.33 ppm (peak Q) are shown in Figure 5. The expected reverse NOE back to UA12 (peak D) can readily be seen. In addition peak N at −12.6 ppm is also cross relaxed and we assign N to GC10. From this experiment alone one might attribute the excitation of N to spillover from imperfectly monochromatic irradiation of Q. On the basis of our experience with the selectivity of the saturating irradiation frequency range, we believe this is not the case. However, two peaks that are close in frequency from base pairs that are also

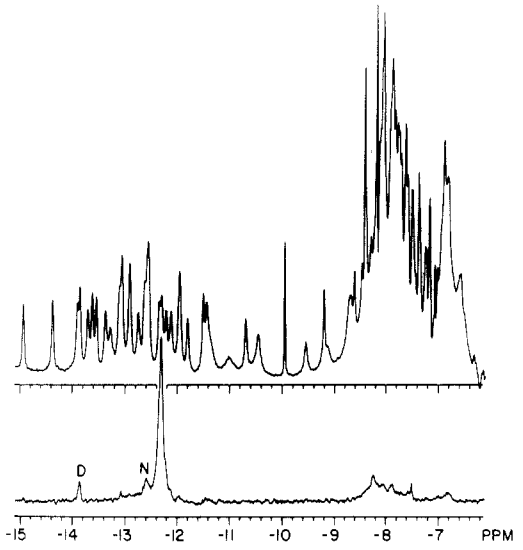

FIGURE 5: Difference NOE spectrum produced by selective saturation of peak Q. Peak Q was saturated for 0.4 s by irradiation slightly on the upfield side of center. The absence of appreciable cross-saturated narrow CH peaks in the upfield aromatic spectrum indicates that peak Q is a GC base pair. The upper spectrum is an unirradiated control spectrum at 23 °C.

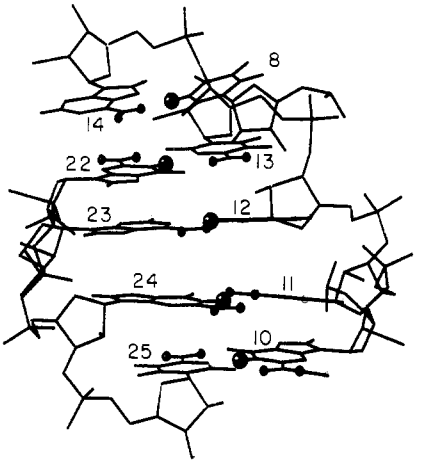

FIGURE 6: Perspective computer graphics projection of the four secondary base pairs in the tRNA D stem and the tertiary 8–14 Hoogsteen base pair stacked on the end of this helix. The coordinates of the crystal structure refined in reciprocal space were used (Sussman et al., 1978), and proton coordinates were generated by a computer program (D. Hare, unpublished). Protons are represented by spheres; the large filled spheres are the low-field nitrogen protons irradiated in this study.

close in space do present special problems in NOE studies. There are, however, four independent lines of evidence indicating that peak N is GC10. First, from the time-dependent spin diffusion experiment in Figure 4, N must be the next-to-nearest neighbor of UA12 (peak D); thus N (−12.6 ppm) must be base pair 14 or base pair 10, but base pair 14 is independently assigned to peak A. Second, Redfield's group could directly assign base pair 10 in yeast $tRNA^{Phe}$ at −12.63 ppm via a methyl to ring NH NOE (Johnston & Redfield, 1981); the D stem sequences of yeast phenylalanine tRNA and *E. coli* valine tRNA are identical except for one methyl group. Third, irradiation either at the center of peak Q or slightly on the upfield side of peak Q cross saturates peak N without exciting peak O; if the effect were spillover, the larger and closer peak O would have been more affected. Fourth, long-term irradiation of peak N, even on the downfield side to minimize spillover, partially saturates peak D via the mediation of peak Q. Thus, the next-to-nearest neighbor relationship of D to N can be demonstrated in the N–Q–D direction as well as in the D–Q–N direction; this corroborates our assignment of peak N to CG10, the next-to-nearest neighbor of UA12 (peak D). Irradiation of peak Q also produces a small effect at peak T. If this is not spillover, it could represent either the 26–44 tertiary pair or CG27; we have not investigated it further.

Discussion

The assumed structure of the D helix of *E. coli* $tRNA_1^{Val}$ based on the crystal structure of the same five base pairs in yeast $tRNA^{Phe}$ is shown in Figure 6; the ring NH protons irradiated in this NOE study are shown as enlarged filled circles. Table I lists the distances from the ring NH of each base pair to surrounding protons according to the crystal coordinates (Sussman et al., 1978); proton coordinates were generated by a computer program using the known N–H and C–H bond angles and bond lengths (D. Hare, unpublished). In the present study the NOE resulting from selective saturation of each ring NH was monitored, starting at the independently assigned s^4U8–A14 proton (peak A). Peak K was determined to be the nearest neighbor to peak A by cross saturation, but further analysis was complicated by the presence of two base pairs (both GC pairs) in peak K. Although irradiation of peak K established that peak D was a nearest neighbor, it was not known which of the two base pairs in K was a neighbor of D. This problem was resolved by taking advantage of spin diffusion. Long-term saturation of A lead to cross saturation of D through K, thus establishing the connectivity A–K–D. Peak D could be connected to peak Q as a nearest neighbor and to peak N as a next-to-nearest neighbor by monitoring the effects of spin diffusion at longer time periods. This then established the connectivity A–K–D–Q–N which leads to the assignment of peak K to CG13, peak D to UA12, peak Q to CG11, and peak N to GC10.

The data can also be analyzed from a different perspective by making use of the narrow aromatic CH NOE to discriminate AU base pairs from GC pairs. From the aromatic NOEs of the linked set A–K–D–Q–N, only A and D are AU pairs and they are next-to-nearest neighbors rather than nearest neighbors. Thus the AU pair D must have a GC pair on either side with an AU pair and a GC pair as next-to-nearest neighbors. There are only two places in *E. coli* $tRNA_1^{Val}$ where this occurs, thus establishing that peak D is either UA4 or UA12. With careful application and well-resolved spectra, the sequential NOE technique can lead to this type of coarse sequence information; at present we cannot distinguish the polarity of adjacent base pairs; i.e., GC pairs are indistinguishable from CG pairs as are AU and UA pairs. Thus, even in the absence of any independent assignments, the NOE data alone reveal the presence of the sequence (AU/UA)-(GC/CG)-(AU/UA)-(GC/CG)-(GC/CG) somewhere in this tRNA.

Careful scrutiny of the crystal structure reveals that the ring NH to ring NH distances for the adjacent base pairs 10–11, 11–12, and 13–14 are all within 3.8 Å and might reasonably be expected to generate direct first-order NOEs at the level of a few percent. However, the ring NHs of base pairs 12 and 13 appear to be separated by 4.7 Å which theory predicts to be too far for even a 1% NOE. There are three possible interpretations for the D to K NOE between UA12 and CG13. One is that the NOE to G22 N1-H is a second-order NOE transmitted from U12 N3-H via the A23 amino protons, both of which are situated within 3.7 Å of G22 N1-H and are ideally located to serve as a conduit for magnetization transfer. However, peak K picks up saturation from peak D quite

rapidly (see Figure 4) which might argue against a second-order effect. A second possibility is that U12 N3-H and G22 N1-H are closer than 4.7 Å and the crystal structure needs minor adjustment (by an amount less than the resolution at which the X-ray data were collected). In this connection it is worth noting that the ring NH to ring NH distances differ when using the Duke, MIT, MRC, or Wisconsin coordinates as the scaffolding for generating proton coordinates (D. Hare, unpublished observations). A third possibility is that the structure in solution under our conditions differs slightly from the crystal structure(s). The X-ray crystals were grown in the presence of magnesium and spermine, whereas our NMR data were obtained under mildly limiting magnesium conditions. Especially noteworthy in this connection is the fact that peak D (UA12) moves downfield onto peak C in the presence of excess magnesium (Reid et al., 1979).

At this point it is illuminating to compare these direct assignments from dipolar coupling with less direct methods involving hairpin fragments, paramagnetic ion broadening, ring-current shifts, etc. published earlier (Lightfoot et al., 1973; Kearns & Shulman, 1974; Reid et al., 1979; Hurd et al., 1979). The previous assignment of peak A at −14.9 ppm to s^4U8–A14 agrees with the K to A NOE and with several independent assignment reports and was in fact the starting point of this study. Previous assignment of UA12 at −13.8 ppm and CG10 at −12.6 ppm (Reid et al., 1979) is in good agreement with their direct assignment by NOE at −13.84 and −12.60 ppm, respectively. The latter also agrees well with the assignment of GC10 at −12.63 ppm by methyl–ring NH NOE in yeast $tRNA^{Phe}$ (Johnston & Redfield, 1981). There is far less agreement, however, in the assignment of CG11 and CG13. In both yeast $tRNA^{Phe}$ and *E. coli* $tRNA_1^{Val}$ CG11 was estimated to be between −13.0 and −13.1 ppm (Kearns & Shulman, 1974; Reid et al., 1979; Johnston & Redfield, 1981). This estimate was based on ring-current shift theory and analysis of D-stem hairpin fragments which are not subject to the extensive tertiary interactions of the D stem in intact tRNA. The present NOE results indicate that CG11 is actually 0.7 ppm further upfield than previous estimates, i.e., at −12.23 ppm instead of −13.05 ppm. It is possible that the structural distortion and helix irregularity introduced by forming the additional tertiary interactions to the D stem secondary base pairs leads to greater than expected upfield shifts on CG11 by neighboring ring currents. However, even using the coordinates of each base from the crystal structure, Robillard et al. (1976, 1977b) estimated a resonance position of −13.1 ppm for CG11; the error may reside in the assumed unshifted starting resonance position of CG11. An even greater disparity was observed for CG13. The NOEs from base pairs 12 and 14 establish that CG13 is at −13.05 ppm, whereas previous estimates from ring-current shifts, fragments, and paramagnetic ion broadening assigned it at either −11.5 or −12.0 ppm (Lightfoot et al., 1973; Kearns & Shulman, 1974; Reid et al., 1979; Hurd et al., 1979). Because of its stacking directly over the G22 N1-H in the early crystallographic data, A14 was assumed to strongly upfield shift the CG13 ring NH in the ring-current estimates; however, refinement of the crystal structure now places A14 where its ring-current shift on CG13 ring NH is quite small. In the isolated D stem fragment the CG13 resonance may well be in the upfield region between −11 and −12 ppm, but this merely points out the problems in attempting to assign intact tRNA resonances, especially at the helix termini, from fragment spectra. It is noteworthy that Robillard et al., using ring currents and the Duke X-ray coordinates, estimated that in intact tRNA CG13 should resonate at −13 ppm in both yeast $tRNA^{Phe}$ and *E. coli* $tRNA_1^{Val}$ (Robillard et al., 1976, 1977b). In the paramagnetic broadening experiments, a resonance at −12.0 ppm was relaxed at the same time the s^4U8–A14 peak broadened (Hurd et al., 1979). Since CG13 is next to s^4U8–A14, it was assigned to the broadened peak at −12.0 ppm on the assumption that the paramagnetic ion occupied a single discrete site near the 8–14 base pair. The assumption of a single binding site at low paramagnetic ion levels now appears to be unjustified. In the light of the present data we would interpret the paramagnetic results as indicating manganese and cobalt ion binding to an additional independent site involving the −12.0-ppm resonance, without knowing the identity of this resonance or this site. The assignment of UA12 is also of interest in connection with the work of others. Johnston et al. (Johnston et al., 1979; Johnston & Redfield, 1981) assigned UA12 at −13.6 ppm (peak F in Figure 1) in *E. coli* $tRNA_1^{Val}$ on the basis of its slow solvent exchange behavior (a similar "slow proton" was also found at −13.65 ppm in yeast $tRNA^{Phe}$). This assignment is in error, and the present NOE assignment of UA12 to peak D at −13.84 ppm, rather than to peak F, indicates that it is not UA12, but some other base pair elsewhere in the molecule, that exhibits very slow breathing.

Finally, some comments are in order about the advantages and general applicability of the step-by-step sequential NOE assignment method. This technique, which simply maps the spatial proximity of a given base pair to its two nearest neighbors, is more direct and far less ambiguous than other assignment methods. The major requirements are a reliable, independently assigned starting resonance and a well-resolved spectrum with as few multiple proton peaks as possible. Even when multiple proton peaks are encountered, one can, with care, follow the path through them by using the time dependence of the spin-diffusion process to selectively pass the magnetization through the complex peak to one neighbor by extended irradiation of the other neighbor. In looking for such small NOEs sensitivity is an obvious advantage in that the time required to attain a given signal-to-noise ratio in the Fourier difference spectrum is correspondingly reduced. At 500 MHz the difference spectra shown in this study each required about 40 min of signal averaging. We are currently attempting to assign the entire low-field NMR spectrum of tRNA solely from the dipolar coupling of each resonance to its nearest neighbors. If successful, these unambiguous assignments should pave the way to a much more rigorous analysis of tRNA dynamics, ligand binding, and unfolding.

Acknowledgments

We thank Susan Ribeiro for purifying the *E. coli* valine tRNA in copious quantities. We also thank Alvin Kwiram for his vision and support in establishing high-resolution NMR at the University of Washington and Gary Drobny for maintaining the NMR spectrometers in such excellent condition. Thanks are also due to the Murdock Foundation for generous NMR instrumentation funds. We also thank Dr. A. G. Redfield for sending us data prior to publication.

References

Bothner-By, A. A. (1979) in *Biological Applications of Magnetic Resonance* (Shulman, R. G., Ed.) p 177, Academic Press, New York.

Crothers, D. M., & Cole, P. E. (1978) in *Transfer RNA* (Altman, S., Ed.) p 196, The MIT Press, Cambridge, MA.

Daniel, W. E., & Cohn, M. (1975) *Proc. Natl. Acad. Sci. U.S.A. 72*, 2582.

Daniel, W. E., & Cohn, M. (1976) *Biochemistry 15*, 3917.
Dubs, A., Wagner, G., & Wuthrich, K. (1979) *Biochim. Biophys. Acta 577*, 177.
Hurd, R. E., & Reid, B. R. (1979a) *Biochemistry 18*, 4005.
Hurd, R. E., & Reid, B. R. (1979b) *Biochemistry 18*, 4017.
Hurd, R. E., Azhderian, E. M., & Reid, B. R. (1979) *Biochemistry 18*, 4012.
Jack, A., Ladner, J. E., & Klug, A. (1976) *J. Mol. Biol. 108*, 619.
Johnston, P. D., & Redfield, A. G. (1978) *Nucleic Acids Res. 5*, 3913.
Johnston, P. D., & Redfield, A. G. (1979) in *Transfer RNA: Structure, Properties and Recognition* (Abelson, J., Schimmel, P. R., & Soll, D., Eds.) p 191, Cold Spring Harbor Press, Cold Spring Harbor, NY.
Johnston, P. D., & Redfield, A. G. (1981) *Biochemistry 20*, 1147.
Johnston, P. D., Figueroa, N., & Redfield, A. G. (1979) *Proc. Natl. Acad. Sci. U.S.A. 76*, 3130.
Geerdes, H. A. M., & Hilbers, C. W. (1977) *Nucleic Acids Res. 4*, 207.
Kalk, A., & Berendsen, H. J. C. (1976) *J. Magn. Reson. 24*, 343.
Kan, L. S., & Ts'o, P. O. P. (1977) *Nucleic Acids Res. 4*, 1633.
Kan, L. S., Ts'o, P. O. P., Sprinzl, M., von der Haar, F., & Cramer, F. (1977) *Biochemistry 16*, 3143.
Kastrup, R. V., & Schmidt, P. G. (1975) *Biochemistry 14*, 3612.
Kastrup, R. V., & Schmidt, P. G. (1978) *Nucleic Acids Res. 5*, 257.
Kearns, D. R., & Shulman, R. G. (1974) *Acc. Chem. Res. 7*, 33.
Kim, S. H. (1976) *Prog. Nucleic Acid Res. Mol. Biol. 17*, 181.
Kim, S. H., Sussman, J. L., Suddath, F. L., Quigley, G. J., McPherson, A., Wang, A., Seeman, N. C., & Rich, A. (1974) *Proc. Natl. Acad. Sci. U.S.A. 71*, 4970.
Klug, A., Ladner, J., & Robertus, J. D. (1974) *J. Mol. Biol. 89*, 511.
Lightfoot, D. R., Wong, K. L., Kearns, D. R., Reid, B. R., & Shulman, R. G. (1973) *J. Mol. Biol. 78*, 71.
Noggle, J. H., & Schirmer, R. E. (1971) *The Nuclear Overhauser Effect: Chemical Applications*, Academic Press, New York.
Poulsen, F. M., Hoch, J. C., & Dobson, C. M. (1980) *Biochemistry 19*, 2597.
Redfield, A. G., & Kunz, S. D. (1979) in *NMR and Biochemistry* (Opalla, S. J., & Lu, P., Eds.) p 225, Marcel Dekker, New York.
Reid, B. R. (1981) *Annu. Rev. Biochem. 50*, 969.
Reid, B. R., Ribeiro, N. S., Gould, G., Robillard, G., Hilbers, C. W., & Shulman, R. G. (1975) *Proc. Natl. Acad. Sci. U.S.A. 72*, 2049.
Reid, B. R., Ribeiro, N. S., McCollum, L., Abbate, J., & Hurd, R. E. (1977) *Biochemistry 16*, 2086.
Reid, B. R., McCollum, L., Ribeiro, N. S., Abbate, J., & Hurd, R. E. (1979) *Biochemistry 18*, 3996.
Rich, A., & RajBhandary, U. L. (1976) *Annu. Rev. Biochem. 45*, 805.
Robillard, G. T., Tarr, C. E., Vosman, F., & Berendsen, H. J. C. (1976) *Nature (London) 262*, 363.
Robillard, G. T., Tarr, C. E., Vosman, F., & Reid, B. R. (1977a) *Biochemistry 16*, 5261.
Robillard, G. T., Tarr, C. E., Vosman, F., & Sussman, J. L. (1977b) *Biophys. Chem. 6*, 291.
Roy, S., & Redfield, A. G. (1981) *Nucleic Acids Res.* (in press).
Sanchez, V., Redfield, A. G., Johnston, P. D., & Tropp, J. (1980) *Proc. Natl. Acad. Sci. U.S.A. 77*, 5659.
Schimmel, P. R., & Redfield, A. G. (1980) *Annu. Rev. Biophys. Bioeng. 9*, 181.
Schmidt, P. G., & Edelheit, E. B. (1981) *Biochemistry 20*, 79.
Shulman, R. G., Hilbers, C. W., Kearns, D. R., Reid, B. R., & Wong, Y. P. (1973) *J. Mol. Biol. 78*, 57.
Sussman, J. L., Holbrook, S. R., Warrant, R. W., Church, G. M., & Kim, S. H. (1978) *J. Mol. Biol. 123*, 607.
Tropp, J., & Redfield, A. G. (1981) *Biochemistry 20*, 2133.
Wagner, G., & Wuthrich, K. (1979) *J. Magn. Reson. 33*, 675.
Wong, K. L., Bolton, P. H., & Kearns, D. R. (1975) *Biochim. Biophys. Acta 383*, 446.